MultiRobot Precise Localization Based on Multisensor Fusion

Rongxin Jiang
The Institute of Advanced Digital Technologies&Instrumentation, Zhejiang University
Zhejiang, P.R China
rongxinj@zju.edu.cn

Yaowu Chen*
The Institute of Advanced Digital Technologies&Instrumentation, Zhejiang University
Zhejiang, P.R China
* is the corresponding author
cyw@mail.bme.zju.edu.cn

***Abstract*—This paper proposes a precise collaborative localization scheme based on multisensor fusion for leader-follower multi-robot group. Each robot of the group is equipped with its own unique sensors and obtains self-localization by fusing two proprioceptive sensors. The lead robot uses the observer information to revise the self-localization of each robot. This paper also proposes a fusion model for the laser scanner and the vision sensor; the lead robot uses the vision sensor to obtain the target bearing by object detection technique, and then fuses the bearing information with the laser distance information to localize the target. Corresponding to the actual usage, this paper have analyzed and resolved the errors which are results of the operation delay, network delay, and other reasons. To validate our proposed scheme, we have implemented a team localization experiment with a Pioneer 3-AT robot and 3 AmigoBot robots. The results verify that our proposed scheme is valid and viable.**

***Keywords*—Multi-Sensors Fusion, Multi-Robots Localization, Extended Kalman Filter**

I. INTRODUCTION

To perform some sensible task, such as Multi-Sensors Fusion, Multi-Robots Localization and Extended Kalman Filter (EKF) autonomous navigation, the multi-robots must have an estimate of its current position. Therefore, the localization is one of the important questions for the multi-robots group. Many people have done some significant research regarding the robot localization which can be classified into a few categories. Some research focus on information fusion with different sensors, [1] fuses sonar and vision sensor information. [2] fuses laser and vision sensor information. Another research attempts to obtain precise localization with different fusion algorithms. [3][4][5] obtain localization information using Extended Kalman Filter, the algorithm can predict non-linear system effectively under Gauss white noise. [6][7] estimate the relative position between each two members of the robot team using maximum likelihood estimation. [8][9] use the ordinary least squares and particle filter method respectively. Moreover, some proposed schemes attempt to research the problem from a form of collaboration: Each robot is equipped with the same set of proprioceptive sensors and exteroceptive sensors, then fuse the proprioceptive data with the exteroceptive data which is obtained by considering the most general relative observation between each of the two robots[5][10]. [11] addresses a leader-follower formation of mobile robots. Throughout this investigation, most research focus on the theory and simulation, and few schemes have proposed an integrated solution and applied to actual usage.

This paper proposes an integrated scheme for the multirobot group. Each robot is equipped with its own unique sensors. All robots localize itself with proprioceptive sensors fusion. The lead robot uses the exteroceptive sensors to obtain the observation information, which can be fused with the proprioceptive data of each robot to revise self-localization. The precise localization can then be determined.

The features of our proposed scheme are as the following:

- Each robot is equipped with its own exteroceptive sensor and works with the leader-follower formation. The lead robot is equipped with a laser and a vision sensor which the other individual robot member isn't equipped for. This mechanism is more realistic for the actual applications.
- Propose a novel sensor fusion form for the laser and vision sensors: We obtain the target bearing with monocular vision sensor based on object detection technique and obtain the target distance information from the laser sensor. Then we can obtain the target localization by fusing the two sensors' information. The fusion mode is different from [1] [2] etc.
- Corresponding to the actual usage, we have analyzed and resolved the errors which are the results of the operation delay, network delay, and others. This paper has performed the relevant experiments to prove the scheme.

The remainder of this paper is organized as follows. Section II introduces the proposed scheme. Section III illustrates the theory of localization and the relevant algorithms. Section IV analyzes and resolves the error. Section V presents the performance evaluations. Section VI summarizes this paper and presents the conclusions.

II. SCHEME

The localization process is composed of the following two phases.

- Initialization phase: The lead robot takes a picture of the target using the vision sensor. The horizontal projection P^t (refer to Fig.4) of the target can be obtained using the

978-1-4244-1674-5/08 /$25.00 ©2008 IEEE

camera calibration technique. Then we can figure out the angle θ_t between P^t and the camera center axis. Based on the angle θ_t and the angle η_k between the camera center axis and the laser center, the distance between the robot and the target can be obtained (refer to Fig.1). With this strategy, the lead robot can localize itself by observing two fixed landmarks. We also can obtain the relative localization of each member robot with the same way.

- Run phase: At run time, each robot localizes itself by fusing the proprioceptive data. The lead robot observes the two landmarks using laser and vision sensors, and fuses the observation data with proprioceptive sensors data. Then revises self-localization in terms of this fusion result. Each member receives the observation information from the lead robot via AD-HOC network, and fuses it with proprioceptive sensors data to revise self-localization.

III. THEORIES AND ALGORITHMS

A. Exteroceptive Sensor Model

1) Laser model

The lead robot is equipped with a Leuze ROD4 laser scanner, which have 190 degree angle of view and 50 meter maximal distance. Each scan unit is 0.36 degree and every scan can get 529 sample points. The laser model can be described as Fig.1.

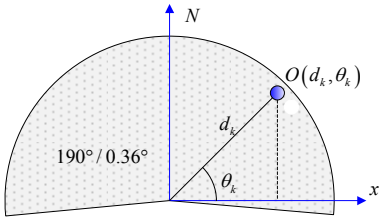

Fig.1 The laser scanner model

N is the laser center bearing, θ_k is the angle between the object O and x horizontal axis. Therefore, the detected object can be expressed with polar coordinate as $(d_k, \theta_k)^T$, or with Cartesian coordinates as

$$u_k = \left(d_k \cos\theta_k, d_k \sin\theta_k\right), k = 1,\ldots, N \qquad (1)$$

2) Sonar array model

Sonar provides direct range information at low cost. Each member robot is equipped with a sonar array, which is composed of 10 densely dispersed sonar sensors; 8 sensors are fixed in the robot head, the rest are fixed in the robot tail. The sonar array can detect target of 120 degree range. The detection distance range is from 15cm to 7 meters. The sonar array model is the same as the laser model, and can be expressed with polar coordinates as $(d_k, \theta_k)^T$.

3) Vision sensor model

In a general pinhole camera model, the relationship between a 3D point $[x,y,z,1]^T$ and its 2D image projection $[u,v,1]^T$ can be represented by the following equation:

$$\begin{bmatrix} u \\ v \\ 1 \end{bmatrix} = \frac{1}{z}\begin{bmatrix} f_{cx} & 0 & c_x & 0 \\ 0 & f_{cy} & c_y & 0 \\ 0 & 0 & 0 & 0 \end{bmatrix}\begin{bmatrix} x \\ y \\ z \\ 1 \end{bmatrix} \qquad (2)$$

f_{cx} and f_{cy} are the two ponderances of the camera's focal length and $(c_x,c_y)^T$ is the principal point of the image. The real camera is affected by lens distortion. The main source of lens distortion is the radial distortion, which is caused by light rays bending. Then the equation (2) can be expressed as,

$$\begin{bmatrix} u \\ v \\ 1 \end{bmatrix} = \frac{1}{z} * \begin{bmatrix} f_{cx} & 0 & c_x & 0 \\ 0 & f_{cy} & c_y & 0 \\ 0 & 0 & 0 & 0 \end{bmatrix}\begin{bmatrix} x \\ y \\ z \\ 1 \end{bmatrix} * \left(1 + k_1 r^2 + k_2 r^4 + k_3 r^6\right) \qquad (3)$$

where k_1,k_2, and k_3 are the radial distortion coefficients, $r^2=(x/z)^2+(y/z)^2$.Following the camera calibration algorithm of [13], the camera's interior parameter f_{cx}, $f_{cy,}$,c_x,c_y, k_1,k_2,k_3 can be obtained. Therefore, the projection of the 3D point $(x_1,y_1,z_1,1)^T$ is $(u_1,v_1,1)^T$ on the virtual image plane (refer to Fig.4). According to equation (3), the new projection point $(u_1^c,v_1^c)^T$ can be formulized as:

$$\begin{bmatrix} u_1^c \\ v_1^c \end{bmatrix} = \frac{1}{\left(1 + k_1 r^2 + k_2 r^4 + k_3 r^6\right)} * \begin{bmatrix} u_1 \\ v_1 \end{bmatrix} \qquad (4)$$

B. Self Localization

Since the precision is very low with the robot navigated by an odometer, the discrete Kalman filter is applied to fuse the odometer with gyroscope data for the linear model. We define state parameter $X= [v_L,v_R,w_g]^T$, The state function is $X_{k+1}=A_{k+1}X_k+w_k$, where A_{k+1} is the state switching matrix is from k to $k+1$ time, and w_k is the process Gauss noise with covariance matrix Q. [12] have used the same proprioceptive sensors model as refering to its state switching matrix: $A = \begin{bmatrix} 1 & 0 & 0 \\ 0 & 1 & 0 \\ -1/\beta D_{RL} & 1/\beta D_{RL} & 0 \end{bmatrix}$; β is the revision coefficient which is obtained by the iterative experiments. The observation function is $Z_k=H_kX_k+v_k$ and the observation value can be obtained from the proprioceptive sensors. Therefore the measure matrix H_k is the identity matrix I.

Fig.2 presents data which the robot is navigated with the fusion of two proprioceptive sensors. The result shows that the fusion navigation is approaching more closely to the real track comparing with the odometer navigation.

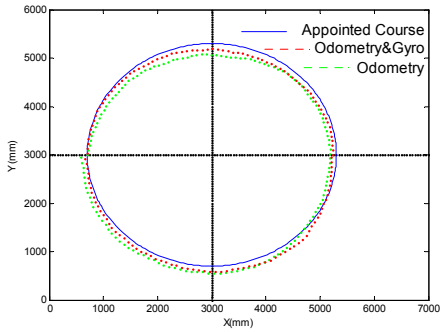

Fig.2 The self-localization course line

C. Fusion Rivision

1) Process model

The Arc model [4] is used to described the navigation state with bearing changing as illustrated in Fig.3,

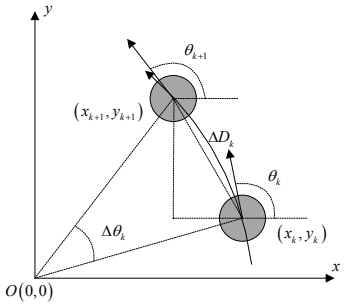

Fig.3 The state model of robot

We define the state parameter $X=[x,y,\theta]^T$, the process model can be deduced as:

$$X_{k+1}=f(X_k,u_k)+\omega_k$$
$$f(X_k,u_k)=\begin{bmatrix} x_k+\frac{\Delta D_k}{\Delta\theta_k}\left(\sin(\theta_k+\Delta\theta_k)-\sin\theta_k\right) \\ y_k-\frac{\Delta D_k}{\Delta\theta_k}\left(\cos(\theta_k+\Delta\theta_k)-\cos\theta_k\right) \\ \theta_k+\Delta\theta_k \end{bmatrix},|\Delta\theta_k|>0 \quad (5)$$

where w_k is the process Gauss noise with covariance matrix Q, $u_k=(\Delta D_k,\delta\theta_k)^T$ is the proprioceptive sensors input, D_k is the arc length and θ_k is the turning angle. The two parameters can be obtained from the fusion result of the proprioceptive sensors.

2) Observation Model

In this subsection, we obtain the observation information of the target from the vision sensor and laser scanner, which is illustrated in subsection *a)*. Then we deduce the observation functions from the observation model in Fig.5.

a) Object detection

From Fig.4, P is the extracted center point of the object, O is the camera model's pinhole, OC_o is the camera center axis, vC_ou is the virtual image plane, $p(u_t,v_t)$ is the projection of P in the virtual image plane, p^t is the projection of p to the axis C_op^t, and P^t is projection of P to the horizontal plane zOx. The relative angle to the recognized object from robot denoted as θ_t at time t. θ_t can be deduced as $\theta_t=\tan^{-1}\left(\frac{\left|width_{image}/2-u_t^c\right|}{width_{image}/2}*\tan\alpha\right)$.

where 2α is the camera's field of view, and $width_{image}\times height_{image}$ is the image's size. Therefore, the object's distance information can be obtained from equation (1) with θ_t.

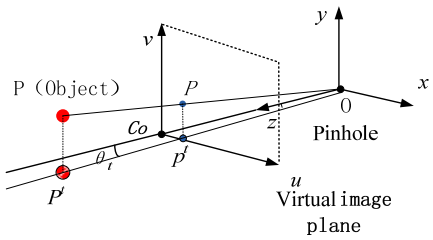

Fig.4 Object detection model

b) Relation model

Since only the position information of the members can be obtained from the observation information from the lead robot, we can only revise the position coordinate of the individual members. The relative model of laser scanner and vision sensor is illustrated as Fig.5.

In Fig.5, *1* is the lead robot, *2* is one of the members and LM_A, LM_B are the fixed landmarks. Black line N is the lead robot course and red line C is the center axis of the camera.

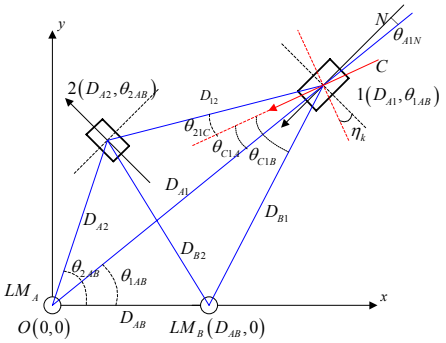

Fig.5 The relation model of multirobot

Some well-defined conditions are declared as the following:

1. A polar coordinate is used to describe the relative position between the robots and the landmarks. The LM_A is set to be the coordinate origin, and the directed line LM_A to LM_B is the positive direction of the coordinate horizontal axis. The distance between LM_A and LM_B is D_{AB};
2. η_k is the angle between C and N. The parameter changes with the Pan, Tilt and Zoom device (PTZ) running, and can be obtained from PTZ directly.

The following metrics represent the naming manner:

1. Segment: Name with the position of the start point and the end point. For instance, D_{AB} is the segment from LM_A to LM_B.
2. Angle: Name with three vertex points, and angle vertex is placed the middle position. For instance, θ_{1AB} is the angle of *1*,*A* and *B* three vertex points.

According to sensors model, the distance parameters which can be obtained from Fig.5 directly are; D_{12},D_{A1},D_{B1}, and the angle parameters are; θ_{21C}, θ_{C1A}, θ_{C1B}. Therefore we can deduce the polar coordinate of the lead robot as

$$(D_{A1},\theta_{1AB})=\left(D_{A1},\arccos\left(\frac{D_{A1}^2+D_{AB}^2-D_{B1}^2}{2D_{A1}D_{AB}}\right)\right).$$

The course of the lead robot is (θ_{1AB}+η_k-θ_{C1A}).

And the polar coordinate of the member can be deduced as

$$D_{A2}=\sqrt{D_{12}^2+D_{B1}^2-2D_{12}D_{B1}\cos(\theta_{21C}+\theta_{C1A})}$$
$$(D_{A2},\theta_{2AB})=\left(D_{A2},\arccos\left(\frac{D_{A2}^2+D_{AB}^2-\left(D_{12}^2+D_{B1}^2-2D_{12}D_{B1}\cos(\theta_{21C}+\theta_{C1B})\right)}{2D_{A2}D_{AB}}\right)\right).$$

c) Observation function

For the member robot, the polar coordinate (D_{A2}, θ_{2AB}) can be transformed to Cartesian coordinate (x_k,y_k). The distance observation function is represented as

$$Z_j^d=H_j^dX_j+v_j^g=\sqrt{(x_k-x_j)^2+(y_k-y_j)^2}+v_j^g \quad (6)$$

where v_j^g is Gauss white noise.

For the lead robot, the polar coordinate (D_{A1}, θ_{2AB}) can be transformed to Cartesian coordinate (x_k,y_k). The distance observation function can be formulized as $Z_k = \sqrt{x_k^2 + y_k^2} + v_d$. The course is $\theta = \theta_{1AB} + \eta_k - \theta_{C1A}$, where θ_{C1A} and η_k are measurable parameters and the observation function of the course can be abbreviated as

$$Z_k^b = H_k^b X_k + v_k^b = \arctan\left(\frac{y_k}{x_k}\right) - \theta + v_k^b \qquad (7)$$

where $v_k{}^b$ is Gauss white noise.

IV. Error Handle

The aforementioned scheme is quite viable in theory. However, corresponding to actual usage, there are some non-negligible errors described in the following.

A. Object Detection Delay

The localization process of monocular vision sensor is composed of three phases: imaging, object detection, and bearing compute. The elapse time of this period is uncertain. The robot will leave from the position which is taking picture and ended in a few angle deviations. Thus, according to the object detection model, there is an error that the distance data is obtained from the laser scanner using this angle.

Since the elapse time of object bearing detection results in the deviated angle, the time cost is determined to be <= 250ms in terms of our experiments. To handle the error, we use the twin imaging method; we place down a colorized column on each member robot, which can be detected within a short time. At the first imaging phase, we snatch the whole robot with object detection algorithms, and mark the rough object field. At the second imaging phase, we only snatch the colorized column image from that field and compute the object bearing. Then we use it to get the distance information from laser scanner data. The second process time would cost about <=40ms. We can figure out the maximal angle deviation is *arctan*[(600*40/1000)/*D*] if assuming the robot move speed <=600ms(refer to the experiment). However, for the target, the scan angle of the laser scanner is *arctan*(*target width* /*D*), where *D* is the distance between the laser scanner and target. In this experiment, the target width is much greater than (600*40/1000)mm. Therefore the problem is solved.

B. Network Delay

The lead robot sends the observation information to the relevant member via AD-HOC network. This process will take some time. The relevant robot would leave from the prior position after receiving the data. Thus, there are some errors that the member fuses the receiving data with its current proprioceptive data.

In our model, the robot moves around origin *O* with radius *R*. As Fig.6 represents, (*x*,*y*) is the actual coordinate of the robot and ($x^{'}$,$y^{'}$) is the estimated position. The robot is observed at position (x_{k1},y_{k1}), then reach the position (x_{k2},y_{k2}) after interval Δt: Δt is equal to the localization time plus the network transmission time.

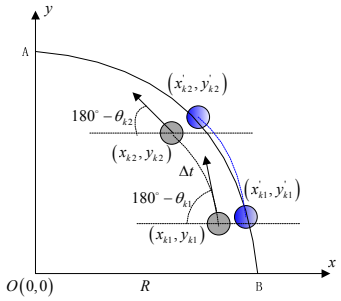

Fig.6 Network delay revision model

Assuming the proprioceptive sensors have *n* times data fusion within Δt, we reserve the state serial $\{X_1, X_2, \ldots, X_m\}$ where $X=\{x,y,\theta\}$,m>n. After receiving the observation information, we fuse it with the data extracted from the reserved series. (x_{k1},y_{k1}) is the estimated position from data fusion. In terms of the proprioceptive sensors model, we can fit an estimated trajectory with the reserved series. Then we deduce the new estimated position $\left(x_{k2}^{'}, y_{k2}^{'}\right)$, which is the actual position that the robot should move to.

The remaining problem is to compute the network transmission time. In this experiment, the network time protocol (NTP) is used to get the synchronous time. The lead robot acts as the NTP server, and the members are the NTP clients. The robots obtain the synchronous time at the initialization phase. The experiment result denotes the precision of the synchronous time is within 10 milliseconds.

C. Observation Blockage

The member self-localization is revised with the observation information. However, the member can't be observed by the lead robot as illustrated in Fig.7 (*R*1 is the lead robot, *R*2 and *R*3 are the members. The course bearing of *R*1 is *N*1 and of *R*2 is *N*2) where three robots are move onto a same straight line, the lead robot has no way to observe *R*3.

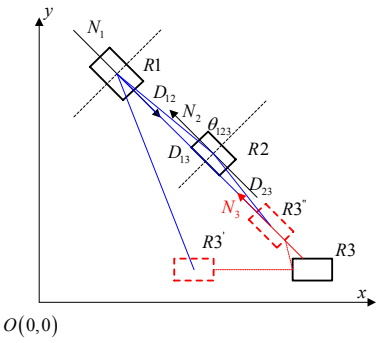

Fig.7 Observation blockage model

This problem would be divided into two cases. The first cases is when *R*3 moving to the position of *R*3' after a period of time. For this case, we navigate *R*3 with its proprioceptive sensor fusion when *R*3 was blocked by *R*2 until *R*3 can be observed. The proprioceptive sensors information would then be discarded. The second case is *R*3 moving to the blocked position of *R*3'', and going forward with the bearing N_3 for a longer period of time. The distance D_{12} between *R*1 and *R*2 is measurable, the distance D_{23} between *R*2 and *R*3'' can be obtained from sonar sensor, and θ_{123} can be determined by the

measurement of the vision sensor. Thus, the distance D_{13} can be deduced as; $\sqrt{D_{12}^2 + D_{23}^2 - 2D_{12}D_{23}\cos\theta_{123}}$.

V. PERFORMANCE EVALUATION

A. Experiment Environment

To validate our proposed scheme, we have implemented a team localization experiment described as the following:

- Robots and sensors

Our multi-robots group is composed of a Pioneer 3-AT and three AmigoBot. Fig.8 represents the lead robot which is equipped with a Leuze ROD4 laser scanner whose capability is referred in the *Laser Model* subsection. The monocular vision sensor is fixed upon the PTZ. Each member robot is equipped with a sonar array whose capability is referred in the *Sonar Model* subsection.

This experiment set the moving speed of the robots is <=600mm per second.

- Experiment scenario

Fig.8 shows the experiment is implemented in a clear indoor field. Two landmarks are placed with fixed height and distance. We paint some colorized lines, circles, and curves as designated course line. Let the members follow the lead robot navigating along the course line. Those robots navigate by estimating their position with multisensors data fusion. We mark down the actual course line which can be used for capability contrast.

- Communication condition

Each robot is equipped with WiFi device which support IEEE 802.11b standard. All robots compose a mobile AD-HOC network.

Fig.8 The experiment scenario

B. Experiment

The whole experiment includes the initialization phase localization and the run time localization. The following metrics are used for the following subsection.

BR: The robot hasn't been revised by the observation information of the lead robot and only navigated by the proprioceptive sensors.

AR: The robot has been revised by the observation information of the lead robot.

1) Initialization localization

Each robot is motionless at this phase and obtains self-position by the observation information of the lead robot. Therefore, the localization precision is relied on the precision of the laser scanner and the vision sensor. The experiment result shows the error is less than 10mm.

2) Run time localization

a) The robots course line

Fig.9 represents the actual course line of the three members along with the designated course. As top right corner describes, the three course lines are corresponding to three members respectively.

As seen from Fig.9, the BR course line obviously deviates from the designated course line during the experimental period. This phenomenon is resulted from the cumulative effects of the proprioceptive sensors. The AR course line deviates less from the designated course line, and does not have the obvious cumulative deviation.

The lead robot course line is represented as Fig.10.

b) The course contrast

To quantifiably illuminate the performance of the proposed scheme, we sample the three course lines every 150mm to record the deviation values in Fig.9 and Fig.10. We have done five data statistics from 5 different experiments and figured out the average value as the illustrated in Fig.11.

As seen from Fig.11, in contrast with BR, the AR has less deviations and no cumulative deviation. The AR deviation of the lead robot is less than the member's; this is because the lead robot appends self deviation when revises the member self-localization with observation information.

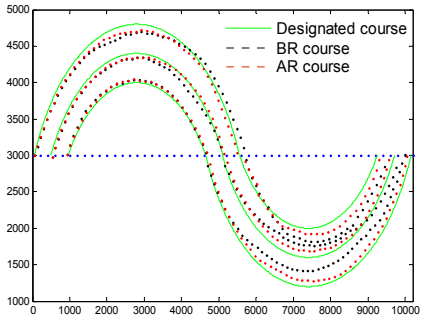

Fig.9 The three members course line

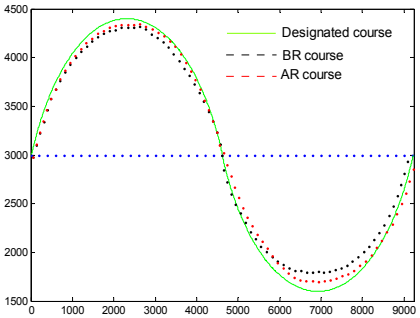

Fig.10 The lead robot course line

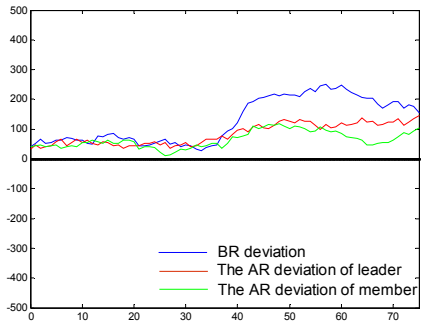

Fig.11 The course deviation contrast

c) Error handling for observer blockage

To validate the proposed strategy for the error handling method for observer blockage, we perform a scenario as in Fig.12.

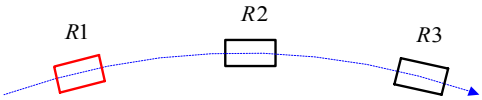

Fig.12 A scenario for error handle

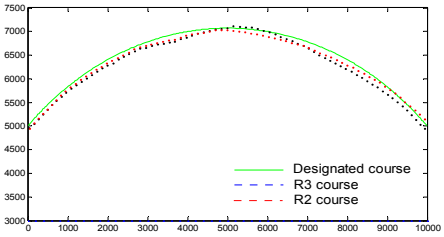

Fig.13 The course line for error handle

The two member robots *R*2 and *R*3 follow the lead robot moving along a determined course line which has a small curvature. *R*3 is blocked by *R*2, the lead robot *R*1 cannot observe *R*3 commonly. The experiment result is illustrated as Fig.13.

Fig.13 shows the course deviation of *R*2 is less than the course deviation of *R*3. This is because R3 obtains the observation information by using the sonar sensor whose precision is less than the laser scanner. However, the deviation of R3 is limited to an acceptable range. The experiment result proves the proposed handling strategy is viable.

VI. CONCLUSION

We have proposed a precise localization scheme for multi-robots group based on multi-sensors' information fusion. Each robot localizes itself using the proprioceptive sensors fusion and then the self-localization is revised by the observation information. The discrete Kalman filter is used to fuse two proprioceptive sensors, and the extended Kalman filter is used to fuse the proprioceptive data with the exteroceptive data. We also have proposed a novel fusion model for the two exteroceptive sensors. The results of our experiment validate that the proposed scheme can achieve precise localization with low error range. Moreover, the error is not cumulative.

REFERENCES

[1] P. Zingaretti , E. Frontoni, Vision and sonar sensor fusion for mobile robot localization in aliased environments, IEEE/ASME International Conference on Mechatronic and Embedded Systems and Applications, MESA 2006, Beijing, China, August 2006.

[2] Arras K.O., Tomatis N., Jensen B., Siegwart R., "Multisensor On-the-Fly Localization: Precision and Reliability for Applications," Robotics and Autonomous Systems, vol. 34, issue 2-3, pp. 131-143, February 2001.

[3] A.I. Mourikis and S.I. Roumeliotis, "Optimal Sensor Scheduling for Resource Constrained Localization of Mobile Robot Formations", IEEE Transactions on Robotics, 22(5), pp. 917-931, Oct. 2006.

[4] Jensfelt, P. and H.I. Christensen, Pose tracking using laser scanning and minimalistic environmental models, IEEE Transaction on Robotics and Automation, 17(2),pp. 138-147, 2001.

[5] Distributed Multirobot Localization S.I. Roumeliotis and G.A. Bekey, 2002, Distributed Multirobot Localization, IEEE Transaction On Robotics And Automation Vol 18, No.5, October 2002

[6] A. Howard, M. J. Mataric, and G. S. Sukhatme, "Localization for mobile robot teams using maximum likelihood estimation," in Proc. IEEE/RSJ Int. Conf. Robot. Intell. Syst., Lausanne, Switzerland, pp. 434–459, Sep.-Oct. 2002.

[7] F. Dellaert, F. Alegre, and E. B. Martinson, "Intrinsic localization and mapping with 2 applications: Diffusion mapping and Marco Polo localization," in Proc. IEEE Int. Conf. Robot. Autom., Taipei, Taiwan, R.O.C., pp. 2344–2349, Sep. 2003.

[8] A. Das, J. Spletzer, V. Kumar, and C. Taylor, "Ad hoc networks for localization and control," in Proc. 41st IEEE Conf. Decision Control, Las Vegas, NV, pp. 2978–2983, 2002.

[9] D. Fox, W. Burgard, H. Kruppa, and S. Thrun, "A probabilistic approach to collaborative multi-robot localization," Auton. Robots, Special Issue Heterogeneous Multirobot Syst., vol. 8, no. 3, pp. 325–344, 2000.

[10] Agostino Martinelli, Frederic Pont, Roland Siegwart: Multi-Robot Localization Using Relative Observations. ICRA 2005: 2797-2802

[11] Gian Luca Mariottini, Fabio Morbidi, Domenico Prattichizzo, George J. Pappas, Kostas Daniilidis: Leader-Follower Formations: Uncalibrated Vision-Based Localization and Control. ICRA 2007: 2403-2408

[12] Zong Guanghua, Deng Luhua, Wang Wei, Robust localization algorithms for outdoor mobile robot, 2007,33(4):454-458

[13] Heikkila , J . Silven , O. A four - step camera calibration procedure with implicit image correction Computer Vision andPattern Recognition [C] .In :1997.Proceedings ,1997 IEEE Computer Society Conference on, 17 - 19 Jun1997 :1106 -1112.

[14] Lienhart R, Maydt J. An Extended Set of Haar-like Features for Rapid Object Detection, IEEE ICIP 2002, Vol. 1, pp 900~903, 2002.

[15] Alexander Kuranov, Rainer Lienhart, and Vadim Pisarevsky. An Empirical Analysis of Boosting Algorithms for Rapid Objects With an Extended Set of Haar-like Features. Intel Technical Report MRL-TR-July02-01, 2002